Vibrational Spectra and Structure of $CH_3Cl:(H_2O)_2$ and $CH_3Cl:(D_2O)_2$ Complexes. IR Matrix Isolation and ab Initio Calculations

Nadia Dozova, Lahouari Krim,* M. Esmaïl Alikhani,* and Nelly Lacome

Université Pierre et Marie Curie-Paris 6, CNRS, LADIR UMR 7075, Boîte 49, 4 Place Jussieu, 75252 Paris, Cedex 05, France

Received: May 24, 2007; In Final Form: July 12, 2007

The infrared spectra of $CH_3Cl + H_2O$ isolated in solid neon at low temperature have been investigated. High concentration studies of water (0.01%−4%) and subsequent annealing lead to the formation of the ternary $CH_3Cl:(H_2O)_2$ complex. Detailed vibrational assignments were made on the observed spectra of water and deuterated water engaged in the complex. In parallel, structural, energetic, and vibrational properties of the complex have been studied at the second-order Møller−Plesset perturbation theory using several basis sets. Anaharmonic correction to the vibrational frequencies has been done with the standard second-order perturbation approach. It was shown that the ground state of the complex has a cyclic form for which the nonadditive three-body contribution was found to be around 10% of the interaction energy.

I. Introduction

Studies of weakly bonded molecular complexes formed between water and atmospheric molecules such as N_2, O_2, CO, and NO can give important information on molecular interactions in atmospheric and astrophysical chemistry. Van der Waals and hydrogen-bonded molecular complexes have motivated both theoretical and experimental studies. Sandler et al.[1] analyzed a weakly bonded cluster of water with nitrogen, combining ab initio calculations of the potential energy surface with diffusion Monte Carlo calculations of the vibrational ground state for different H_2O-N_2 isotopic species. Coussan et al.[2] investigated the infrared spectra of the $H_2O + N_2$ reaction in argon matrix. They identified several $(H_2O)_m(N_2)_n$ species such as H_2O-N_2 and $(H_2O)_2-N_2$. The structural properties of these two complexes are discussed on the basis of calculations, carried out within the framework of density functional theory (DFT). Hirabayashi et al.[3] reported IR absorption bands of $(H_2O)_2-(N_2)_n$ complexes isolated in solid argon. In several studies water trimer has been the subject of intensive investigations.[4,5] Arunan et al.[6] investigated the rotational-tunneling spectra of $Ar-(H_2O)_2$ and $Ar-(D_2O)_2$. The structure of the gas phase of $(H_2O)_2-CO_2$ complex was determined through an analysis of rotational spectra of different isotopically substituted species by Peterson et al.[7] Rode et al.[8] determined from the supermolecular calculations the energetic properties of the $(H_2O)_2-CO$ ternary complex. The 2:1 complexes between water and trans and cis isomers of nitrous acid have been investigated by Obert-Majkut et al.[9] using argon matrix isolation and DFT calculations.

In the course of parallel investigations in this laboratory where we focused on studies of binary complexes[10−13] of H_2O with other molecules of stratospheric significance, it is interesting to compare the evolution of structural and electronic properties which can be inferred from the spectral data for the next complexation step with a second water molecule, the more stable species $CH_3Cl:(H_2O)_2$. In the present study, the structure of the two isotopic species of $CH_3Cl:(H_2O)_2$ and $CH_3Cl:(D_2O)_2$ complexes were investigated by neon matrix isolation combined with infrared absorption spectroscopy. Detailed vibrational assignments were made from the observed spectra of $H_2O + CH_3Cl$ and $D_2O + CH_3Cl$ systems. Using ab initio calculations, geometric and vibrational properties of these complexes have been estimated.

II. Experimental Technique

$CH_3Cl + H_2O$ samples were prepared by co-condensing $CH_3Cl/H_2O/Ne$ mixtures onto a cryogenic metal mirror maintained at 5 K. Molar ratios (X/Ne; X = CH_3Cl or H_2O) ranged from 0.001% to 4%. The experimental method and setup have been previously described in detail.[14] We shall recall only the main points. Deposition times were around 60 min. Neon and CH_3Cl gases were obtained from L'Air liquide with purities of 99.9995% and 99.8%, respectively. CH_3Cl was purified by using trap-to-trap vacuum distillations. Deuterium isotopic water (Euriso-top 99.90%) as well as natural water was degassed in a vacuum line. The purity of samples was confirmed spectroscopically.

Infrared spectra of the resulting samples were recorded in the transmission-reflection mode between 4500 and 500 cm^{-1} using a Bruker 120 Fourier transform infrared (FTIR) spectrometer equipped with a KBr/Ge beamsplitter and a liquid N_2 cooled narrow band HgCdTe photoconductor. A resolution of 0.1 cm^{-1} was used. Bare mirror backgrounds, recorded from 4500 to 500 cm^{-1} prior to sample deposition, were used as references in processing the sample spectra. The mirror was at the same temperature as the matrix when the background was collected. However, there is no difference between spectra obtained with the background at 5 or 300 K. We also tried to use pure neon matrix as a background, but no difference was observed in the sample spectra. Absorption spectra in the midinfrared were collected on samples through a KBr window mounted on a rotatable flange separating the interferometer vacuum (10^{-3} mbar) from that of the cryostatic cell (10^{-7} mbar). Next, or after sample annealing up to 12 K in several steps, infrared spectra of the samples were recorded again between 4500 and 500 cm^{-1}. The spectra were subsequently subjected

* Corresponding authors. E-mail: krim@ccr.jussieu.fr (L.K.); ea@spmol.jussieu.fr (M.E.A.).

10.1021/jp074028+ CCC: $37.00
Published on Web 09/15/2007

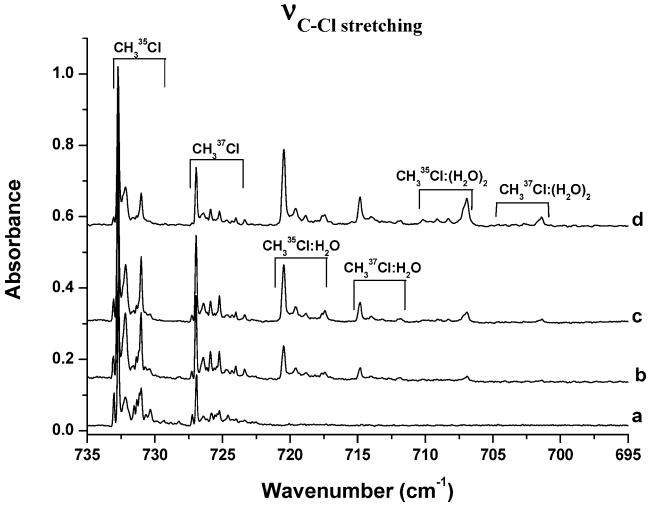

Figure 1. Effects of H_2O concentration on 1:1 and 1:2 $CH_3Cl:H_2O$ bands in the C−Cl stretching ($\nu_{3\ CH_3Cl}$) region of CH_3Cl: (a) $CH_3Cl/Ne = 5/10000$; (b) $CH_3Cl/H_2O/Ne = 5/1/10000$; (c) $CH_3Cl/H_2O/Ne = 5/2/10000$; (d) $CH_3Cl/H_2O/Ne = 5/5/10000$. Spectra were recorded at 5 K after annealing to 12 K.

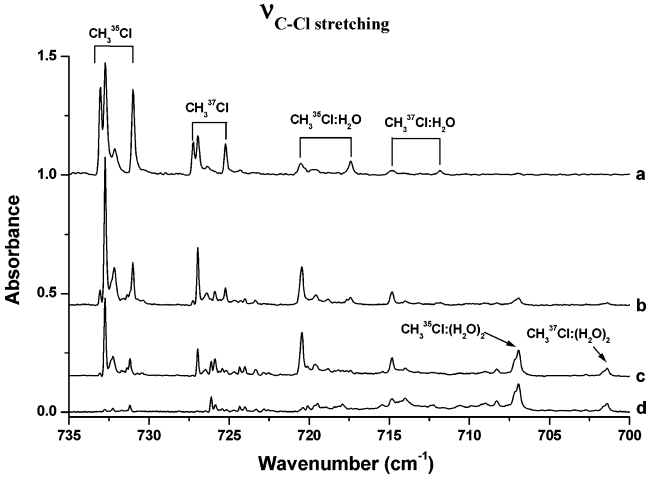

Figure 2. Annealing effects on 1:1 and 1:2 $CH_3Cl:H_2O$ bands in the C−Cl stretching ($\nu_{3\ CH_3Cl}$) region of CH_3Cl: (a) after deposition at 5 K; (b) after annealing to 7 K; (c) after annealing to 12 K; (d) after annealing to 13 K. All spectra were recorded at 5 K.

to baseline correction to compensate for infrared light scattering and interference patterns. All spectra were recorded at 5 K. For each sample, corresponding to different concentrations of CH_3Cl and H_2O, two kinds of spectra were recorded at 5 K, after each of the following procedures: (1) after sample deposition; (2) after warming the matrix at several steps up to 13 K in order to vary and monitor the formation of higher stoichiometry complexes. The heating of the matrix depends a lot on how the system is isolated, on the configuration of pumping, and on the intermediate steps of heating to reach a temperature. In our case we managed to heat up to 13 K and to have always matter to analyze. An important loss of the matrix is observed only starting from 14 K.

III. Experimental Results

H_2O + CH_3Cl in Ne Matrix. Upon co-deposition of a mixture $H_2O/CH_3Cl/Ne$, new bands appear in the vibrational regions of both CH_3Cl and H_2O, in addition to those attributed to unreacted CH_3Cl, H_2O, and $(H_2O)_2$ species. These bands are assigned to complexes between H_2O and CH_3Cl.

CH_3Cl in Ne Matrix. Spectra of pure CH_3Cl isolated in neon matrixes have been recorded at 5 K at different concentrations of CH_3Cl and have been previously described.[15] In the following we will take the C−Cl stretching spectral region as a characteristic domain of the specific vibrational modes of CH_3Cl monomer, $CH_3Cl:H_2O$ complex, and $CH_3Cl:(H_2O)_2$ complex. Briefly, the C−Cl stretching region (Figure 1a) has two sets of bands belonging to the two isotopomers $CH_3{}^{35}Cl$ and $CH_3{}^{37}Cl$. Each band consists of sharp peaks due to splitting by the matrix cage. As already reported, the peaks for the most stable site of CH_3Cl are situated at 732.7 cm^{-1} for $CH_3{}^{35}Cl$ and 726.9 cm^{-1} for $CH_3{}^{37}Cl$, as shown in Figures 1 and 2.

As described in ref 13, bands that grow linearly with the concentrations of both CH_3Cl and H_2O are assigned to the complex $CH_3Cl:H_2O$. When the experiments were carried at very low concentrations of H_2O and CH_3Cl in neon matrix, in order to limit the aggregation processes, $CH_3Cl:H_2O$ bands became predominant. When CH_3Cl is deposited with relatively concentrated H_2O/Ne mixtures, strong absorptions are observable near 700 and 706 cm^{-1} (see Figure 1). These presented a clear second-order dependence with the water concentration and a marked growth after annealing the sample to promote molecular diffusion. The relative intensity of 3:1 between the two bands indicates that the band at 706.9 cm^{-1} belongs to the $CH_3{}^{35}Cl:(H_2O)_2$ isotopomer, while the band at 701.4 cm^{-1} belongs to $CH_3{}^{37}Cl:(H_2O)_2$.

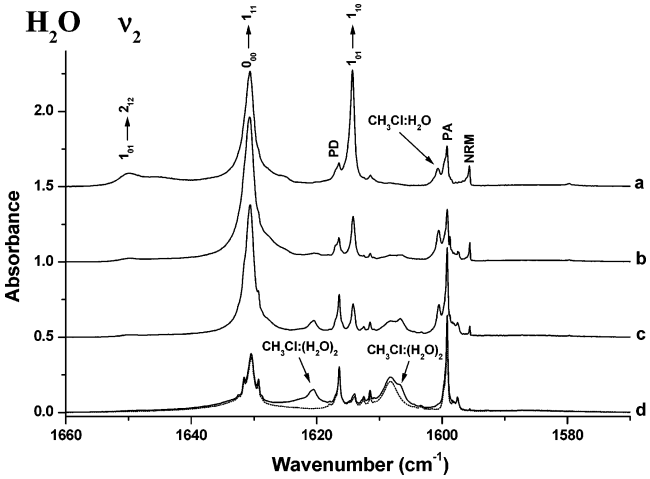

Figure 3. Annealing effects on 1:1 and 1:2 $CH_3Cl:H_2O$ bands in the HOH bending mode (ν_2) region of water: (a) after deposition at 5 K; (b) after annealing to 7 K; (c) after annealing to 12 K; (d) after annealing to 13 K. All spectra were recorded at 5 K. —, $CH_3Cl/H_2O/Ne = 5/1/10000$; ---, $H_2O/Ne = 1/10000$. PA, proton acceptor; PD, proton donor; NRM, nonrotating monomer.

The annealing of the matrix allows the formation of the complex $CH_3Cl:H_2O$, but also the formation of complexes of greater size, such as $CH_3Cl:(H_2O)_2$. Figure 2 shows the evolution of the bands of the complex in the C−Cl stretching mode region. Upon annealing between 5 and 11 K, $CH_3Cl:H_2O$ bands increase. They remain constant or slightly decrease at 12 K in order to form higher stoichiometry complexes such as $CH_3Cl:(H_2O)_2$ species (band observed at 706.9 and 701.4 cm^{-1}). At 13 K all the bands of $CH_3Cl:H_2O$ complex (and those of CH_3Cl monomer) have disappeared. The intensity of the band of $CH_3Cl:(H_2O)_2$ remains constant while other bands (assigned to $CH_3Cl:(H_2O)_n$ ($n \geq 3$)) increase at 715 cm^{-1}. This fact allows the differentiation between 1:1, 1:2, and 1:n ($n \geq 3$) $CH_3Cl:(H_2O)_n$ complexes. The characteristic bands of the $CH_3Cl:H_2O$ complex increase upon annealing to 11 K, decrease upon annealing to 12 K, and fully disappear upon annealing to 13 K. The bands of $CH_3Cl:(H_2O)_2$ increase between

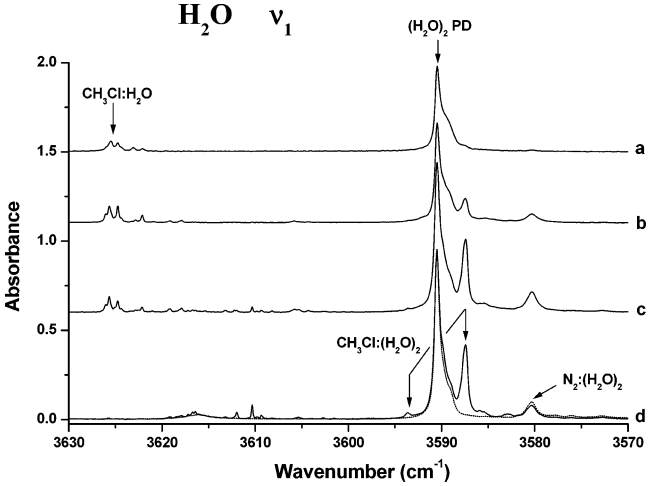

Figure 4. Annealing effects on 1:1 and 1:2 $CH_3Cl:H_2O$ bands in the symmetric OH stretching mode (ν_1) region of water: (a) after deposition at 5 K; (b) after annealing to 7 K; (c) after annealing to 12 K; (d) after annealing to 13 K. All spectra were recorded at 5 K. —, $CH_3Cl/H_2O/Ne = 5/1/10000$; ---, $H_2O/Ne = 1/10000$. $N_2:(H_2O)_2$ is observed after matrix annealing. N_2 exists as an impurity in neon matrix.

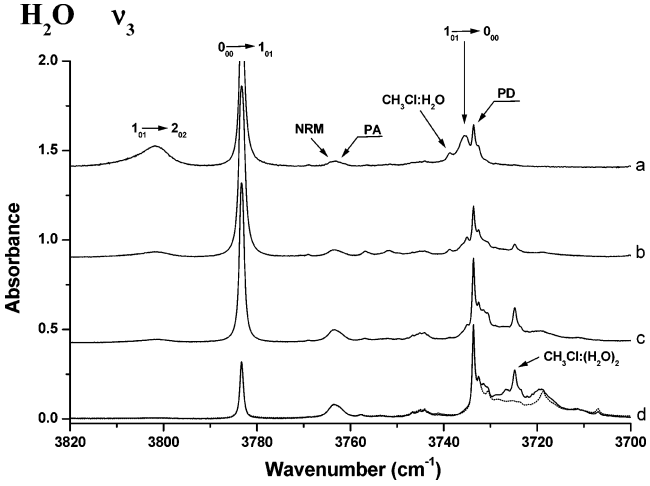

Figure 5. Annealing effects on 1:1 and 1:2 $CH_3Cl:H_2O$ bands in the antisymmetric OH stretching mode (ν_3) region of water: (a) after deposition at 5 K; (b) after annealing to 7 K; (c) after annealing to 12 K; (d) after annealing to 13 K. All spectra were recorded at 5 K. —, $CH_3Cl/H_2O/Ne = 5/1/10000$; ---, $H_2O/Ne = 1/10000$.

5 and 12 K and remain constant between 12 and 13 K, while aggregates such as $CH_3Cl:(H_2O)_n$ appear after annealing to 13 K.

H_2O Vibrational Regions. Water molecules isolated in a rare gas matrix have the particularity of rotating inside the matrix cage, and thus the rovibrational spectrum of water monomers can be observed.[16−20] Thus the H_2O rovibrational transitions (labeled $J'_{K''a\,K''c} \rightarrow J'_{K'a\,K'c}$) of the rotating monomer (RM) give rise to several rovibrational lines. Other water molecules are trapped in matrix sites where their rotation is strongly hindered. These nonrotating monomers (NRMs) give rise to transitions close to the pure vibrational frequencies. The three vibrational fundamentals of H_2O NRM are situated at 1595.6 cm^{-1} (HOH bending ν_2), at 3665.5 cm^{-1}(symmetric stretching ν_1), and at 3761.1 cm^{-1} (antisymmetric stretching ν_3).[13]

The effect of annealing upon the bands in the HOH bending (ν_2), O−H symmetric stretching (ν_1), and O−H antisymmetric stretching (ν_3) regions are given in Figures 3, 4, and 5, respectively. Upon annealing to 13 K the band of $CH_3Cl:H_2O$ disappears while the intensities of bands attributed to $CH_3Cl:(H_2O)_2$ complex remain constant.

The ν_2, ν_1, and ν_3 bands of the $CH_3Cl:H_2O$ complex are situated at 1600.5, 3625.9, and 3738.8 cm^{-1}, respectively. In the $CH_3Cl:(H_2O)_2$ complex case, almost to each water monomer vibrational mode ν_i ($i = 1, 2, 3$) corresponds two absorption signals: the ν_2 bands at 1606.6 and 1620.5 cm^{-1}, the ν_1 bands at 3527.8 and 3587.5 cm^{-1}, and finally the ν_3 band at 3725.1 cm^{-1}. The ν_1 band at 3587 cm^{-1} is formed by two peaks at 3587.5 and 3590 cm^{-1}, due to the trapping sites in the neon matrix.

All vibrational mode frequencies and shifts of $CH_3Cl:H_2O$ and $CH_3Cl:(H_2O)_2$ ($\nu_{complex} - \nu_{monomer}$) are summarized in Table 1.

$CH_3Cl + D_2O$ in Ne Matrix. *C−Cl Region.* Infrared spectra for different samples with $CH_3Cl/H_2O/Ne$ and $CH_3Cl/D_2O/Ne$ in the C−Cl stretching region are shown in Figure 6. As already reported, the bands for the most stable site of the $CH_3Cl:(H_2O)_2$ complex are situated at 706.9 cm^{-1} for $CH_3{}^{35}Cl:(H_2O)_2$ and 701.4 cm^{-1} for $CH_3{}^{37}Cl:(H_2O)_2$, as shown in Figure 6. The bands of $CH_3Cl:(D_2O)_2$ have the same structure as the bands

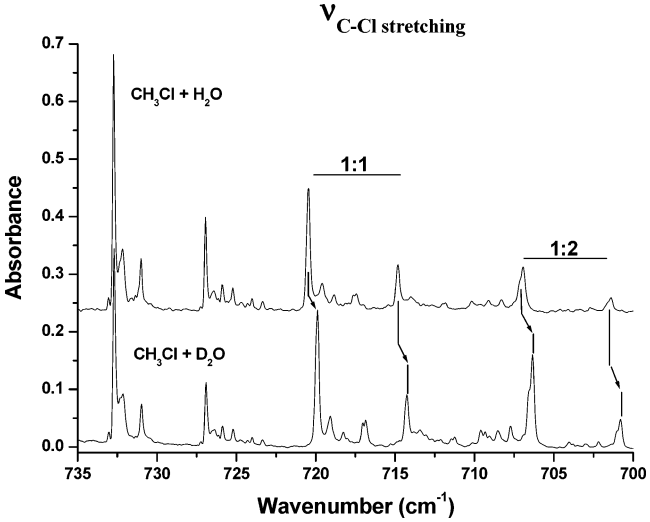

Figure 6. C−Cl stretching ($\nu_{3\,CH_3Cl}$) region of $CH_3Cl + H_2O$ and $CH_3Cl + D_2O$ samples after annealing to 12 K: (a) $CH_3Cl/H_2O/Ne = 5/2/10000$; (b) $CH_3Cl/D_2O/Ne = 5/2/10000$.

of $CH_3Cl:(H_2O)_2$, but are slightly red-shifted; thus the bands of the most stable site of $CH_3Cl:(D_2O)_2$ are located at 706.4 cm^{-1} for $CH_3{}^{35}Cl:(D_2O)_2$ and 700.9 cm^{-1} for $CH_3{}^{37}Cl:(D_2O)_2$.

D_2O Region. D_2O spectral regions are similar to those of H_2O. However, they are spectrally more compact due to the smaller rotational constant of D_2O.[21] Figure 7 shows the ν_2 D_2O spectral region of $CH_3Cl/D_2O/Ne$ mixture after annealing to 12 K. The most intense peak of rotating D_2O molecules is situated at 1199.3 cm^{-1} ($1_{00} \rightarrow 1_{11}$ states). Another intense peak at 1181.2 cm^{-1} belongs to the proton acceptor[21] (PA) of $(D_2O)_2$. Two new bands, located at 1185.9 and 1193.7 cm^{-1}, are attributed to $CH_3Cl:(D_2O)_2$ species. They behave like the bands at 700.9 and 706.4 cm^{-1} in the C−Cl region, assigned to $CH_3Cl:(D_2O)_2$ complex, with regard to water and CH_3Cl concentrations and matrix annealing.

All vibrational mode frequencies and shifts of $CH_3Cl:(D_2O)_2$ ($\nu_{complex} - \nu_{monomer}$) are summarized in Table 2.

IV. Theoretical Calculations

All geometry optimizations and force field calculations have been performed by using the second-order Møller−Plesset

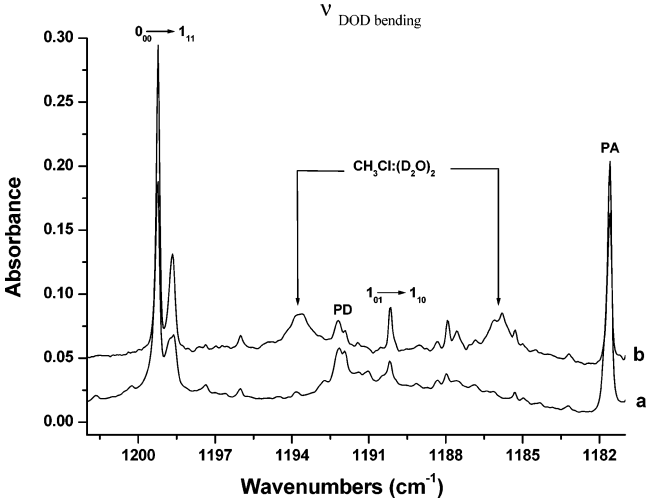

Figure 7. DOD bending (ν_2) region of D_2O and $CH_3Cl:(D_2O)_2$ complex after annealing to 12 K: (a) D_2O/Ne = 2/10000; (b) CH_3Cl/D_2O/Ne = 5/2/10000.

perturbation theory (MP2), as implemented in the Gaussian 03 package,[22] with the aug-cc-pVDZ[23] and 6-311++G(2d,2p)[24−26] basis sets. In order to confirm the calculated results, the most stable complex has been also investigated using MP2 method with the triple-ζ basis set of Dunning (aug-cc-pVTZ).

Geometric and Energetic Analysis. Ternary molecular clusters containing two water molecules have been the subject of numerous theoretical studies (water trimer,[4,5] $(H_2O)_2:CO_2$ complex,[7,27] the $(H_2O)_2:N_2$ complex[2] {noncyclic}, and the $(H_2O)_2$:HCl trimer, $(H_2O)_2$:CO hydrogen-bonded complex[8]). These works evidenced two important points concerning the geometric and energetic characteristics of the ternary complexes:

(i) Over several local minima (stationary points), in the majority of ternary complexes the most stable geometry corresponds to a cyclic form presenting double or triple hydrogen bonds.

(ii) In addition to the study of the interaction energy into pair-additive terms (as in the binary complexes), one has to take into account the three-body nonadditive contributions to the stability of the ternary complexes. The three-body cooperative effect on the decomposition of the interaction energy has been recently nicely reintroduced in the ternary H-bonded complexes by Sadlej and co-workers.[8,29]

In the case of the ternary system studied here, $CH_3Cl:(H_2O)_2$, three geometries have been considered on the intermolecular potential energy surface: cyclic, linear, and bifid structures (see Figure 8). In Table 3 are reported dissociation energies with respect to free monomers (CH_3Cl and H_2O) calculated with the MP2 method and using three different basis sets. D_e is equilibrium dissociation energy, whereas D_0 and D_0^{CP} denote the dissociation energy including the zero-point vibrational energy (ZPE) and the basis set superposition error (BSSE) corrections, respectively. The BSSE correction has been done using the prescription of Boys and Bernardi.[30] Geometry optimization followed by frequency calculations showed that three stationary points correspond to local minima on the potential energy surface. As shown in Table 3, the cyclic structure is more stable than the linear and bifid ones by 7 and 10 kJ/mol, when including ZPE and BSSE corrections, respectively. We note that the D_0^{CP} value obtained with the larger aug-cc-pVTZ basis set is slightly larger than that obtained with the smaller aug-cc-pVDZ set. This feature has been already noted by Rode and Sadlej for $(H_2O)_2-CO$.[8] They considered it as a general trend arising from an underestimation of the dispersion in the binding energies of van der Waals complexes by ca. 5−10% at the MP2/aug-cc-pVTZ level of theory.[8]

In the most stable geometry of the $CH_3Cl:(H_2O)_2$ complex (structure 1), water proton acceptor (in water dimer subunit) interacts with the chlorine atom as a proton donor, whereas the water proton donor interacts with a hydrogen atom of CH_3Cl as a proton acceptor. In the other two structures, one of the two water molecules interacts with the methylchlorine molecule as well as a proton acceptor and a proton donor. The most interesting structural parameters, calculated with MP2, are reported in Figure 8. The inter- and intramolecular distances calculated with the three used basis sets do not present any significant dependency on the basis sets. However, on the basis of the MP2/aug-cc-pVTZ results, we observe two kinds of geometric changes in the ternary complexes compared to the dimers: intra- and intermolecular changes. The intramolecular bond lengths almost present a small increase, while the intermolecular distances decrease when going from dimer to trimer. Three significant geometric changes appear during the formation of the ternary complex. The first change concerns H-bonding within the water dimer subunit, namely the O−O distance. Compared to the isolated water dimer (2.910 Å), the O−O bond length decreases in structure 1 (2.824 Å) while it is left almost unchanged in structure 2 (2.908 Å). Two other changes concern the H-bonding between CH_3Cl and water molecules. The O···H distance (O of water and H of methyl-

TABLE 1: Vibrational Mode Frequencies (in cm^{-1}) of CH_3Cl, H_2O (Nonrotating Monomer, NRM), $CH_3Cl:H_2O$, and $CH_3Cl:(H_2O)_2$ Complexes in Neon Matrix

mode		monomer/Ne	$CH_3Cl:H_2O$/Ne	shift[a]	$CH_3Cl:(H_2O)_2$/Ne	shift[a]
CH_3Cl						
C−Cl stretching	$\nu_{3\ CH_3Cl}$	726.9 (^{37}Cl)	714.8	−12.1	701.4	−25.5
		732.7 (^{35}Cl)	720.5	−12.2	706.9	−25.8
C−Cl rocking	$\nu_{6\ CH_3Cl}$	1019.5	1022.2	2.7	1025.2	+5.7
					1033.3	+13.8
C−H symmetric bending	$\nu_{2\ CH_3Cl}$	1354.8	1357.3	2.5	1365.1	+10.3
C−H antisymmetric bending	$\nu_{5\ CH_3Cl}$	1449.6	1455.2	5.6	1458.9	+9.3
					1448.8	−0.8
C−H symmetric stretching	$\nu_{1\ CH_3Cl}$	2967.5	2972.2	4.7	2979.8	+12.3
C−H antisymmetric stretching	$\nu_{4\ CH_3Cl}$	3036.7	3044.2	7.5	3061.7	+25.0
H_2O						
O−H bending	$\nu_{2\ H_2O}$	1595.6	1600.5	4.9	1606.9	+11.0
					1620.5	+24.9
O−H symmetric stretching	$\nu_{1\ H_2O}$	3665.5	3625.9	−39.6	3527.8	−137.7
					3587.5	−78.0
O−H antisymetric stretching	$\nu_{3\ H_2O}$	3761.1	3738.8	−22.3	3725.1	−36.0

[a] Shift = $\nu_{complex} - \nu_{free\ molecule}$.

TABLE 2: Vibrational Mode Frequencies (in cm^{-1}) of CH_3Cl, D_2O (Nonrotating Monomer, NRM), and $CH_3Cl:(D_2O)_2$ Complex in Neon Matrix

mode		monomer/Ne	$CH_3Cl:(D_2O)_2$/Ne	shift[a]
CH_3Cl				
C−Cl stretching	$\nu_{3\ CH_3Cl}$	726.9 (^{37}Cl)	700.9	−26.0
		732.7 (^{35}Cl)	706.4	−26.3
C−Cl rocking	$\nu_{6\ CH_3Cl}$	1019.5	1025.3	+5.8
			1033.7	+14.2
C−H symmetric bending	$\nu_{2\ CH_3Cl}$	1354.8	1365.3	+10.5
C−H antisymmetric bending	$\nu_{5\ CH_3Cl}$	1449.6	1459.2	+9.6
			1448.6	−1.0
C−H symmetric stretching	$\nu_{1\ CH_3Cl}$	2967.5	2980.3	+12.8
C−H antisymmetric stretching	$\nu_{4\ CH_3Cl}$	3036.7	3061.7	+25.0
D_2O				
O−D bending	$\nu_{2\ D_2O}$	1178.8	1185.9	+7.1
			1193.7	+14.9
O−D symmetric stretching	$\nu_{1\ D_2O}$	2676.7	2595.8	−80.9
			2627.1	−49.6
O−D antisymetric stretching	$\nu_{3\ D_2O}$	2785.9	2756.9	−29.0
			2764.4	−21.5

[a] Shift = $\nu_{complex} - \nu_{free\ molecule}$.

TABLE 3: MP2 Energetic Properties, in kJ/mol, for Three Studied Structures with Split-Valence and Correlated Double- and Triple-ζ Basis Sets[a]

	6-311++G(2d,2p)		aug-cc-pVDZ		aug-cc-pVTZ	
	D_e	D_0/D_0^{CP}	D_e	D_0/D_0^{CP}	D_e	D_0/D_0^{CP}
structure 1	49.2	33.5/28.2	51.4	36.0/28.8	49.7	34.5/30.0
structure 2	37.6	24.8/21.7	39.6	26.7/21.6	38.1	*b*
structure 3	30.5	20.7/17.4	34.5	23.6/18.7	32.6	*b*

$E_{2B} + E_{3B} = E_{int}$[c]

	6-311++G(2d,2p)	aug-cc-pVDZ	aug-cc-pVTZ
structure 1	−36.3 − 4.3 = −40.6	−36.8 − 4.4 = −41.2	−40.0 − 4.8 = −44.8
structure 2	−30.9 − 0.1 = −31.0	−30.9 − 0.6 = −31.5	−34.8 + 0.6 = −34.2
structure 3	−24.7 + 0 = −24.7	−25.4 − 0.1 = −25.5	−29.0 + 0.4 = −28.6

[a] Dissociation energies are labeled as D_e (at equilibrium structure), D_0 (including ZPE), and D_0^{CP} (corrected for BSSE). [b] Not calculated. [c] E_{2B} and E_{3B} are the two- and three-body contributions in the interaction energy (E_{int}).

TABLE 4: MP2 Frequency at the Harmonic (First Values) and Anharmonic (Second Values) Framework Using the Three Basis Sets[a]

mode	structure 1			structure 2	structure 3
	6-311	DZ	TZ	DZ	DZ
H_2O stretches	3940/3757(183)	3895/3708(187)	3907	3927/373	3918/3723
	3935/3750(185)	3892/3703(189)	3901	3862/3675	3916/3721
	3769/3599(170)	3726/3548(178)	3730	3797/3619	3773/3592
	3697/3547(150)	3633/3481(152)	3643	3700/3549	3771/3590
CH_3 stretches	3244/3109(135)	3236/3095(141)	3229	3237/3093	3243/3098
	3243/3098(145)	3229/3082(147)	3227	3226/3079	3236/3089
	3125/3025(100)	3103/2990(113)	3108	3105/2988	3109/2992
H_2O bends	1688/1629(59)	1649/1600(49)	1656	1647/1598	1632/1572
	1668/1613(55)	1628/1586(42)	1633	1623/1578	1628/1575
CH_3 bends	1525/1477(48)	1488/1442(46)	1524	1478/1443	1475/1444
	1511/1470(41)	1476/1435(41)	1511	1472/1435	1473/1436
	1423/1384(39)	1381/1350(31)	1413	1373/1347	1376/1348
	1067/1041(26)	1054/1028(26)	1070	1052/1029	1059/1033
	1055/1033(22)	1040/1020(20)	1057	1037/1018	1045/1023
Cl−C stretch	729/677(52)	724/698(26)	740	736/722	720/708
lib PD H_2O	720/609(111)	709/590(119)	709	650/491	321/167
lib PA H_2O	519/438(81)	501/428(73)	502	418/368	299/164

[a] 6-311, DZ, and TZ represent 6-311++G(2d,2p), aug-cc-pVDZ, and aug-cc-pVTZ basis sets, respectively. The anharmonic corrections are reported in parentheses.

chlorine) varies as 2.282, 2.359, and 2.444 Å for structures 1, 2, and 3, respectively. Compared to the O···H bond length in the binary $CH_3Cl:H_2O$ complex (2.436 Å),[13] we note that the shortest O···H distance was found in structure 1. Finally, the H···Cl bond length (H of water and Cl of methylchlorine) has been found to vary as 2.348, 2.548, and 2.487 Å in structures 1, 2, and 3, respectively. All the geometric changes with respect to two isolated dimers, $CH_3Cl:H_2O$ and $(H_2O)_2$, present an additional stabilizing effect in the ternary cyclic complex. In the two other structures the cooperative nature of the intermolecular interaction should be almost out because of the very small geometric changes when going from dimers to trimers. In order to quantify the cooperative effect, we have decomposed the interaction energy according to the strategy suggested in refs 8 and 29:

$$E_{3B} = E_{int}(ABC) - [E_{2B}(AB) + E_{2B}(BC) + E_{2B}(AC)]$$

where E_{2B} and E_{3B} are the two- and three-body contributions in the interaction energy (E_{int}), respectively. MP2 results with

TABLE 5: Experimental and MP2 Frequency Shifts (in cm^{-1}) of the Cyclic $CH_3Cl:(H_2O)_2$ Complex[a]

		MP2		
mode	exptl	6-311++G(2d,2p)	aug-cc-pVDZ	aug-cc-pVTZ
C−Cl stretch	−25.8	−22.0 (−58.8)	−25.2 (−35.4)	−25.0
C−Cl rocking	13.8	19.9 (12.2)	8.4 (13.1)	20.0
	5.7	7.1 (5.0)	8.0 (5.0)	7.2
C−H_3 sym bend	10.3	11.9 (8.0)	12.6 (7.6)	12.0
C−H_3 asym bend	9.3	14.0 (4.8)	15.8 (5.9)	13.3
	−0.8	−0.4 (−2.5)	3.5 (−0.8)	−0.1
C−H sym stretch	12.3	−3.6 (9.1)	−1.0 (5.8)	−2.8
C−H asym stretch	25.0	5.8 (16.0)	12.2 (18.5)	7.3
	N.O.[b]	5.4 (5.8)	5.5 (5.5)	4.9
HOH bend	24.9	27.8 (28.5)	27.2 (28.4)	27.6
	11.0	7.1 (12.0)	6.4 (14.2)	5.1
O−H sym stretch	−78.0	−91.8 (−80.9)	−78.0 (−73.8)	−92.4 (PA)[c]
	−137.7	−164.2 (−133.7)	−171.5 (−141.1)	−179.0 (PD)
O−H asym stretch	N.O.[b]	−45.7 (−40.2)	−46.6 (−41.0)	−47.0 (PD)
	−36.0	−40.6 (−33.8)	−43.0 (−36.6)	−41.5 (PA)

[a] For the MP2 values, the frequency shifts corrected for the effect of the anharmonicity are given in parentheses for two basis sets. [b] Nonobserved band. [c] PA (proton acceptor) and PD (proton donor) are defined with respect to $(H_2O)_2$ subunit in the ternary cyclic complex.

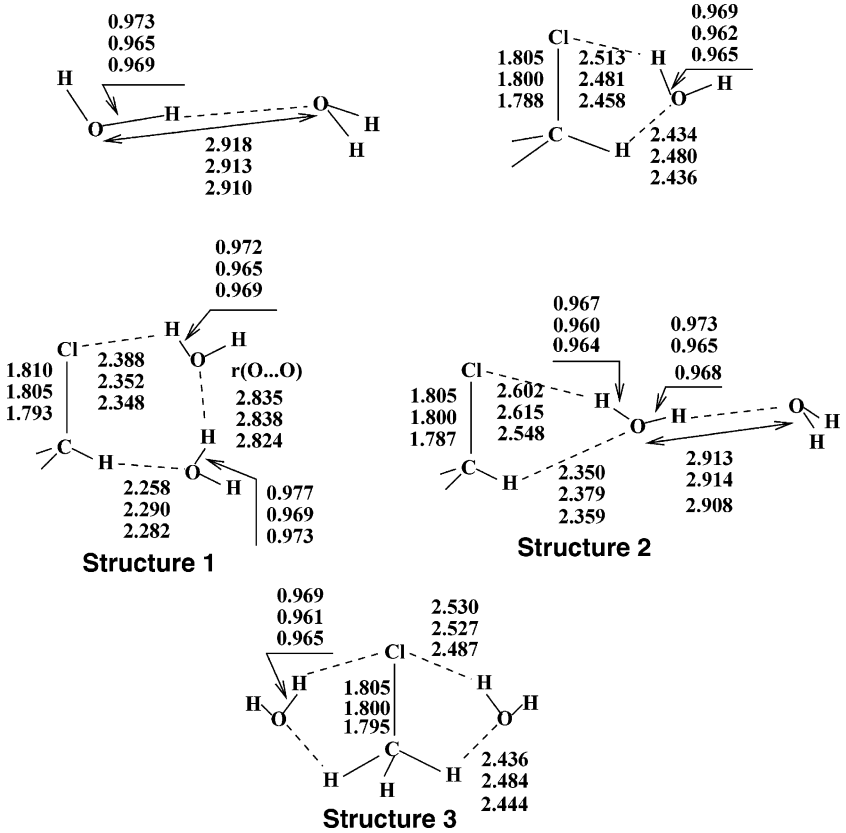

Figure 8. Some significant geometric parameters (in Å) of different studied structures calculated with MP2 using three basis sets: aug-cc-pVDZ (first line), 6-311++G(2d,2p) (second line), and aug-cc-pVTZ (third line).

three basis sets are reported in Table 3. The results clearly show that the three-body nonadditive contribution strongly depends on the hydrogen bond topology. We note the importance of the cooperative stabilization (10%) for structure 1, while the interaction energies of structures 2 and 3 are almost equal to the global pair interactions. The nonadditive contribution for structure 1 is similar to that of the $(H_2O)_2CO$ complex (9%).[8]

Vibrational Study of $CH_3Cl:(H_2O)_2$. All the intramolecular and some of the dimeric intermolecular frequencies, calculated with MP2 at the harmonic approximation, for three geometries are presented in Table 4. The anharmonic frequencies obtained at the MP2 level using the standard second-order perturbation approach have been also reported in Table 4. Inspection of the results shows that the calculated harmonic vibrational frequencies for the cyclic structure are very similar for the three basis sets. The same feature holds valid for the anharmonic vibrational frequencies for all the normal modes, except for the Cl−C stretching mode, for which the anharmonic effect calculated with the split 6-311++G(2d,2p) basis set is twice that calculated with the correlated aug-cc-pVDZ basis. This overestimation of the anharmonicity leads to an exaggerated frequency shift when comparing to the isolated methylchlorine molecule (vide infra).

In order to compare the theoretical results with the experimental ones, we gathered the frequency shifts on the intramolecular modes of the cyclic structure in Table 5. Frequency shifts were calculated with respect to the isolated H_2O and CH_3Cl molecules. For the MP2 values, frequency shifts have been also corrected for the anharmonic effect for two basis sets.

We note that the perturbational anharmonic effects on the frequency shifts globally improve the results compared to the experimental values. Nevertheless, some points merit discussion in more detail:

(1) In the case of the CCl stretching mode, the frequency shift obtained at the harmonic approximation with three basis sets is in good agreement with the experimental value, whereas the perturbative anharmonic effect exaggerates this shift particularly at the MP2/6-311++G(2d,2p) equilibrium which corrupts the shift in lowering it greatly (from -22 to -58.8 cm^{-1}). In inspecting the force constant matrix obtained at the MP2/6-311++G(2d,2p) level, it has been seen that the C−Cl stretching mode ($\nu_{CCl} = 729.8$ cm^{-1}) is calculated too close to one of the libration modes of $(H_2O)_2$ fragment (δ(OH libration) $= 720.5$ cm^{-1}) so that this leads to a strong coupling between two considered oscillators (45.5 cm^{-1}, the most important one in the matrix of anharmonic constants). This issue is partially resolved when using one of Dunning's correlated basis sets (aug-cc-pVDZ; $\nu_{CCl} = 724.8$ and δ(OH libration) $= 709.6$ cm^{-1}). Nevertheless, it should be noted that a perturbative approach is not very well adapted to such nearly degenerate modes to treat exactly the anharmonic effect.

(2) In the case of CH_3 asymmetric bend, the red and blue shifts (9.3 and -0.8 cm^{-1}) are quite well reproduced at the anharmonic framework.

(3) In the case of C−H stretching modes, the significant role played by the anharmonicity on the vibrational frequencies should be underlined. Indeed, the anharmonic effect clearly corrects the sign of the frequency shift in the case of C−H symmetric stretching, and it actually improves the absolute value of the frequency shift for the C−H asymmetric stretching.

(4) In the HOH bending and H−O stretching regions, we have to again point out the significant improvement brought by anharmonicity on the frequency shifts when comparing with the experimental ones. It is interesting to note that two H-bonded cyclic complexes ($CO(H_2O)_2$ and $CH_3Cl(H_2O)_2$) have similar energetic and vibrational features. We have also found that the frequency shifts of the O−H symmetric and asymmetric modes obtained for the $CH_3Cl(H_2O)_2$ complex (-141, -74, -37, and -42 cm^{-1}; see Table 5) are close to those of $CO(H_2O)_2$ (-127, -55, -37, and -36 cm^{-1}).[8]

Finally, in agreement with the recent work of Shield and coworkers[31] on the water clusters, the MP2/aug-cc-pVDZ anharmonic frequencies compare best against experiment with a relatively low cost. Nevertheless, in full agreement with Sadlej[32] and Hobza,[33] we believe that calculations at a higher level of theory, such as the coupled-cluster approach, using a larger basis set (such as aug-cc-pVTZ) will undoubtedly improve the theoretical results.

V. Conclusion

In the present work, the spectroscopic properties of the $CH_3Cl(H_2O)_2$ trimer have been experimentally and theoretically investigated. Observation of two intramolecular spectral regions allowed us to detect the stretching and bending modes of water and methylchlorine partners. The potential energy surface of the ternary complex has been studied using the MP2 approach. Three structures have been studied: cyclic, linear, and bifid forms. Energetically, the global minimum corresponds to the cyclic form. The nonadditive three-body interaction contribution in the interaction energy was found to be around 10% for the cyclic structure and to be negligible for the other two structures. We have found that the structural and energetic properties calculated with the three used basis sets are close to each other.

Vibrational analysis at the harmonic approximation followed by the anharmonic correction done with a perturbative approach has been compared to the experimental data. We showed the following:

(1) Three basis sets give similar vibrational spectra at the harmonic approximation.

(2) For the anharmonic corrections, the use of the correlated double-ζ basis set (aug-cc-pVDZ) is enough good to be parallel to the experimental data at a low cost of calculation, while the split-valence 6-311++G(2d,2p) basis set corrupts the anahrmonic frequency for the C−Cl stretch mode and consequently largely overestimates its shift with respect to the free molecule.

References and Notes

(1) Sandler, P.; Oh, Jung J.; Szczesniak, M. M.; Buch, V. *J. Chem. Phys.* **1994**, *101*, 1378.

(2) Coussan, S.; Loutellier, A.; Perchard, J. P.; Racine, S.; Bouteiller, Y. *J. Mol. Struct.* **1998**, *471*, 37.

(3) Hirabayashi, S.; Ohno, K.; Abe, H.; Yamada, K. M. T. *J. Chem. Phys.* **2005**, *122*, 194506.

(4) Ceponkus, J.; Karlström, G.; Nelander, B. *J. Phys. Chem. A* **2005**, *109*, 7859.

(5) Engdahl, A.; Nelander, B. *J. Chem. Phys.* **1987**, *86*, 4831.

(6) Arunan, E.; Emilsson, T.; Gutowsky, H. S. *J. Chem. Phys.* **2005**, *116*, 4886.

(7) Peterson, K. I.; Suenram, R. D.; Lovas, F. J. *J. Chem. Phys.* **1991**, *94*, 106.

(8) Rode, M. F.; Sadlej, J. *Chem. Phys. Lett.* **2001**, *342*, 220.

(9) Olbert-Majkut, A.; Mielke, Z.; Tokhadze, K. G. *Chem. Phys.* **2002**, *280*, 211.

(10) Loewenschuss, A.; Givan, A.; Nielsen, C. J. *J. Mol. Struct.* **1997**, *408*, 533.

(11) Chaban, G. M.; Gerber, R. B.; Janda, K. C. *J. Phys. Chem. A* **2001**, *105*, 8323.

(12) Dozova, N.; Krim, L.; Alikhani, M. E.; Lacome, N. *J. Phys. Chem. A* **2005**, *110*, 11617.

(13) Dozova, N.; Krim, L.; Alikhani, M. E.; Lacome, N., *J. Phys. Chem. A* **2005**, *109*, 10273.

(14) Danset, D.; Manceron, L. *J. Phys. Chem. A* **2003**, *107*, 11324.

(15) Dozova, N.; Krim, L.; Alikhani, M. E.; Lacome, N. *J. Phys. Chem. A* **2005**, *109*, 10880.

(16) Perchard, J. P. *Chem. Phys.* **2001**, *273*, 217.

(17) Engdahl, A.; Nelander, B. *J. Chem. Phys.* **1989**, *91*, 6604.

(18) Michaut, X.; Vasserot, A. M.; Abouaf, M. L. *Vib. Spectrosc.* **2004**, *34*, 83.

(19) Coussan, S.; Roubin, P.; Perchard, J. P. *Chem. Phys.* **2006**, *324*, 527.

(20) Knözinger, E.; Wittenbeck, R. *J. Am. Chem. Soc.* **1983**, *105*, 2154.

(21) Forney, D.; Jacox, M. E.; Thompson, W. E. *J. Mol. Struct.* **1993**, *157*, 479.

(22) Frisch, M. J.; Trucks, G. W.; Schlegel, H. B.; et al. *Gaussian 03*, revision C.02; Gaussian, Inc.: Pittsburgh, PA, 2003.

(23) Dunning, T. H., Jr. *J. Chem. Phys.* **1989**, *90*, 1007.

(24) Krishnan, R. J.; Binkley, S.; Seeger, R.; Pople, J. A. *J. Chem. Phys.* **1980**, *72*, 650.

(25) Clark, T.; Chandrasekhar, J.; Spitznagel, G. W.; Schleyer, P. v. R. *J. Comput. Chem.* **1983**, *4*, 294.

(26) Frisch, M. J.; Pople, J. A.; Binkley, J. S. *J. Chem. Phys.* **1984**, *80*, 3265.

(27) Nguyen, M. T.; Hegarty, A. F. *Theochem. Phys.* **1987**, *150*, 319.

(28) Kisiel, Z.; Białkowska-Jaworska, E.; Pszczółkowski, L.; Milet, A.; Struniewicz, C.; Moszynski, R.; Sadlej, J. *J. Chem. Phys.* **2000**, *112*, 5767.

(29) Weimann, M.; Fárník, M.; Suhm, M. A.; Alikhani, M. E.; Sadlej, J. *J. Mol. Struct.* **2006**, *790*, 18.

(30) Boys, S. F.; Bernardi, F. *Mol. Phys.* **1970**, *19*, 553.

(31) Dunn, M. E.; Evans, T. E.; Kirschner, K. N.; Shields, G. C. *J. Phys. Chem. A* **2006**, *110*, 303.

(32) Rode, M. F.; Sadlej, J. *Chem. Phys. Lett.* **2003**, *369*, 754.

(33) Pluháčková, K.; Jurečka, P.; Hobza, P. *Phys. Chem. Chem. Phys.* **2007**, *9*, 755.